Compact Self-Shielding Components for Beamforming Networks Implemented in Substrate Integrated Coaxial Line Technology

Laura Van Messem, *Student Member, IEEE,* Arno Moerman, *Student Member, IEEE,* Olivier Caytan, *Member, IEEE,* Hendrik Rogier, *Senior Member, IEEE,* and Sam Lemey, *Member, IEEE*

***Abstract*—A substrate integrated coaxial line (SICL) technology implemented in standard printed circuit board (PCB) technology is proposed to realize shielded miniaturized millimeterwave (mmWave) components, eliminating spurious feed network radiation that may influence the antenna array's radiation pattern. Additionally, coupling to neighboring signal lines is avoided by the self-packaging characteristic of SICL lines, thereby minimizing undesired crosstalk in the routing network. A thorough comparison to more traditional transmission lines, such as grounded co-planar waveguides (GCPWs), shows excellent packaging behavior by minimizing radiation and increasing the routing flexibility between the compact functional components. Further validation of this technology is done by implementing several essential components for beamforming networks: a coaxial via transition, a packaged hybrid coupler and an improved, miniaturized hybrid coupler with direct interfacing. The proposed shielded coaxial via transition from SICL to SICL exhibits a measured insertion loss smaller than 0.74 dB in a broad operational frequency range from 23.75 GHz to 32.5 GHz (31%), covering the n257, n258 and n261 5G bands. In this frequency range, the (miniaturized) SICL hybrid coupler has a measured amplitude imbalance below 1 dB (0.8 dB) and the phase imbalance does not exceed 6° (3°). The proposed miniaturized SICL hybrid coupler has a footprint of only 4 mm in diameter.**

***Index Terms*—5G, grounded co-planar waveguide (GCPW), hybrid coupler, millimeterwave (mmWave), packaged, standard PCB manufacturing, substrate integrated coaxial line (SICL).**

I. Introduction

NAVIGATING the landscape of ever-expanding wireless connectivity, where an explosion in data signals dominates the spectral future, proper packaging becomes a paramount aspect of system design. Careful spatial planning of components and employing self-packaged implementation techniques stand as pivotal challenges for unlocking the full potential of the Internet of Everything (IoE) and future joint-communication and sensing (JCAS) 6G applications [1]. Therefore, an increased focus on inter-component and intra-component electromagnetic interference (EMI)/ electromagnetic compatibility (EMC) considerations becomes essential to ensure reliable functionality of all systems. When targeting higher datarates and finer resolutions, it becomes essential to move up in the frequency spectrum, where the increased path loss ushers the use of larger antenna arrays to obtain more gain. In this respect, special care must be devoted to minimizing spurious radiation from elaborate routing networks to efficiently distribute broadband millimeterwave (mmWave) signals to tens or even hundreds of antenna elements. Minimizing the inter-antenna element coupling to avoid scan blindness [2], as well as maximizing the transmit (Tx)-to-receive (Rx) isolation in full duplex systems [3], remain equally important. Questions arise on how to compactly package this multitude of subsystems.

Traditional coaxial lines and rectangular waveguides (RWGs) yield most favorable shielding properties [4], but are difficult to integrate with standard printed circuit board (PCB) manufacturing. Substrate integrated waveguide (SIW) offers an interesting solution, but remains a bulky alternative. Therefore, grounded co-planar waveguide (GCPW) [5] or stripline [6], [7] topologies are generally favored as compact solutions with reduced spurious radiation. Furthermore, GCPW and stripline technology can be combined to realize compact, low-loss substrate integrated coaxial lines (SICLs) with good power handling capabilities [8]. It presents an attractive solution for packaged systems, owing to its thin profile and excellent shielding, since it is a planar version of a coaxial line. However, conventional SICL implementations employ more elaborate multi-layered PCB technology [9]–[11].

Compact passive multi-beam networks have received a significant amount of attention as an energy-efficient and low-complexity alternative for active beamforming integrated circuits (ICs). To this end, Butler [12]–[14] and Nolen matrices [15]–[17] have been proposed, among other solutions. The implementation of beamsteering networks often relies on a combination of fundamental building blocks, such as a crossover and a hybrid coupler. Miniature crossovers often consist of multi-layer designs [18]. Several miniaturization techniques for hybrid couplers have been proposed in literature below mmWave frequencies [19]–[24]. However, upscaling these designs towards mmWave frequencies and beyond proves cumbersome when aiming for PCB-compatible implementations, as a result of increasingly stringent fabrication limits and tolerances.

This paper proposes a novel, cost-effective manufacturing

Manuscript received February 09, 2024; revised July 26, 2024. This work was partially funded by the Flemish Research Foundation (FWO) and partially by Methusalem.

All authors are with the IDLab-Electromagnetics Group, Department of Information Technology, Ghent University/imec, 9052 Ghent, Belgium. (e-mail: laura.vanmessem@ugent.be; arno.moerman@ugent.be; olivier.caytan@ugent.be; hendrik.rogier@ugent.be; sam.lemey@ugent.be).

procedure for SICLs, based on the assembly of multiple cost-effective single-layer PCBs, fabricated with standard manufacturing technology and compatible with assembly techniques as presented in [25]. Signal lines are locally soldered to obtain galvanic contact, significantly reducing the cost while not compromising the shielding nor increasing undesired spurious radiation. We have designed, fabricated and characterized several fundamental components for beamsteering and routing networks to validate our advocated solution. These include a coaxial via transition interconnecting a pair of SICLs integrated on different layers, a packaged self-shielding hybrid coupler, and an improved miniaturized hybrid coupler. The coaxial via transition provides decoupling of the signal traces with respect to the 3D-GCPW transition of [26]. Additionally, our proposed SICL-to-SICL transition is suited for advanced routing networks, whereas the GCPW-to-SICL transition is preferred for chip interfacing.

This manuscript substantially expands the conference paper [27] by investigating the loss mechanisms of GCPW and SICL more into depth, considering several trace and gap width combinations that are matched to $50\,\Omega$. Furthermore, the extended manuscript showcases a novel packaged miniaturized hybrid coupler, which leverages the compact SICL technology to obtain a footprint of only $4\,\mathrm{mm}$ in diameter. Owing to its excellent component-to-routing isolation, the component allows incoming feed lines from any direction.

The remainder of this paper is organized as follows. In Section II, we introduce the proposed fabrication technology. Section III first performs an elaborate comparison between GCPW and SICL transmission line technology. Thereafter, a transition from SICL to SICL is proposed. Our design is analyzed and compared to measurements. Next, two quadrature hybrid coupler implemented in SICL technology, including a transition from SICL to GCPW for measurement purposes, are presented. In Section IV, the conclusion summarizes the measured performance of all aforementioned components.

II. SICL-Based Packaging Technique

To avoid EMI/EMC problems, the development of reliable mmWave systems requires self-shielded packaging of components that may generate undesired radiation, inter-antenna element coupling or crosstalk in the routing network. In this respect, this section describes a cost-effective manufacturing procedure for compact and self-shielded mmWave components implemented in SICL technology. Specifically, the analysis focuses on the operating frequencies from $20\,\mathrm{GHz}$ to $35\,\mathrm{GHz}$, thus including several important mmWave 5G bands, being the n257 band (26.5-$29.5\,\mathrm{GHz}$), the n258 band (24.25-$27.5\,\mathrm{GHz}$), and the n261 band (27.5-$28.35\,\mathrm{GHz}$).

We propose stacking multiple single-layer PCBs manufactured through standard fabrication, as an alternative for the multi-layer approach in [25]. As shown in Fig. 1, the proposed manufacturing procedure implements the SICL technology by means of two single-layer PCBs, based on a $0.254\,\mathrm{mm}$-thick RO4350B high-frequency laminate with $35\,\mu\mathrm{m}$-thick conductor layers, including an electroless nickel immersion gold (ENIG) surface finish. The bottom PCB (PCB 1) contains

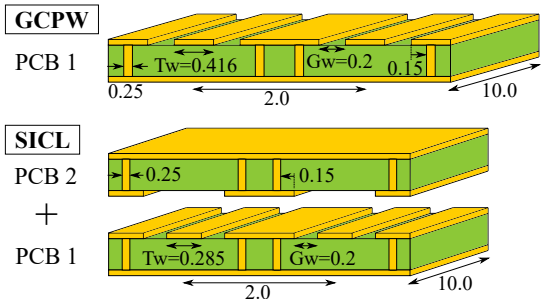

Fig. 1. (top) Layout with dimensions indicated in millimeter of two parallel GCPW lines, consisting solely of PCB 1 and (bottom) two self-shielded SICL lines by assembling PCB 1 and PCB 2.

a traditional GCPW signal line with adjacent ground planes at both sides, connected to the bottom ground plane by rows of vias, $0.25\,\mathrm{mm}$ in diameter, and spaced by a center-to-center distance of $0.5\,\mathrm{mm}$ to suppress field leakage in the frequency range under consideration [28]. Another PCB (PCB 2), with identical grounding structures but without the signal conductor, is then added on top of the GCPW-PCB (PCB 1). Both PCBs are aligned and assembled by means of screws and bolts. As proof of concept, the signal lines' transitions to other layers are locally manually soldered and reflowed to ensure galvanic contact. The assembly of both PCBs results in a total thickness of $0.648\,\mathrm{mm}$ for the SICL line implementation.

Packaging passive components by using our advocated SICL transmission line technology avoids EMI/EMC problems by eliminating radiation and undesired coupling, while maintaining all the advantages of GCPW technology. The technology exhibits good power handling capabilities [8], while keeping the footprint small. Since the fields are concentrated around the signal conductor, radiation and crosstalk between adjacent lines are minimized, as shown in the next section. Compared to their GCPW variants, an additional advantage of the SICL technology, introduced by the increased effective relative permittivity, is the miniaturization of all components.

III. Functional Components

This sections starts with a thorough comparison between two routing technologies: GCPW and SICL. Additionally, as essential building blocks for beamsteering networks [12]–[14], two important passive mmWave components are implemented in SICL technology, being a multi-layer transition for routing and a hybrid coupler to obtain correct phase shifts. Finally, a miniaturized hybrid coupler with improved component-to-routing isolation is presented with a footprint smaller than $4\,\mathrm{mm}$ in diameter. All simulations are carried out using the frequency domain solver of full-wave simulator CST Microwave Studio.

A. GCPW Compared to SICL

The advantages of the proposed packaging solution are highlighted by comparing the performance of traditional GCPW interconnects with the proposed SICL transmission lines. To this end, two adjacent $1\,\mathrm{cm}$-long lines are spaced $2\,\mathrm{mm}$ apart. The GCPW is matched to $50\,\Omega$ by employing a trace width

(Tw) of 0.416 mm, while the SICL requires a trace width of only Tw = 0.285 mm for matching, owing to its increased effective relative permittivity. Both lines have a fixed gap width of Gw = 0.2 mm between the signal conductor and the ground planes next to it. All ground patterns are connected to the bottom ground plane by vias of diameter 0.25 mm, spaced at 0.25 mm from each other and located at 0.15 mm from the copper edge. The simulation model of Fig. 1, including a surface roughness of $R_a = 300\,\text{nm}$ (based on surface roughness measurements of prototypes), yields the scattering parameters shown in Fig. 2.

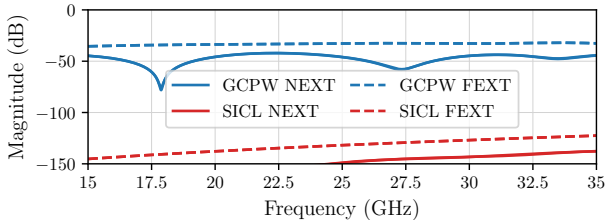

Fig. 2. Comparison of NEXT and FEXT crosstalk in parallel GCPW (solid) and SICL (dashed) lines of 10 mm long with 2 mm separation.

The SICL exhibits a significant overall improved performance in terms of NEXT and FEXT by more than 80 dB. Furthermore, the reflection coefficient of the GCPW remains below −30 dB, while the SICL's reflection coefficient remains below −40 dB. This results in transmission line losses between 0.15 dB at 15 GHz and 0.45 dB at 35 GHz for the GCPW lines, while this is reduced in case of SICL technology: 0.15 dB at 15 GHz to 0.3 dB at 35 GHz.

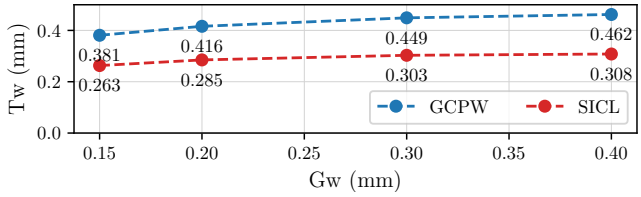

Fig. 3. Trace width (Tw) required to match GCPW and SICL transmission lines to 50 Ω as a function of the gap width (Gw), illustrating the miniaturization effect.

As illustrated in Fig. 3, several trace width (Tw) and gap width (Gw) combinations lead to a 50 Ω characteristic impedance for the GCPW and SICL, with each combination offering a different trade-off in terms of footprint and robustness against fabrication tolerances. It can be concluded that, for each considered gap width, the SICL is slightly miniaturized with respect to the GCPW as a result of the increased effective relative permittivity. The trace and gap widths considered in Fig. 3 are used to perform the loss analysis in Fig. 4, which report the percentage of conductor loss, dielectric loss and radiation loss of both the GCPW and SICL configurations introduced in Fig. 1. For both the GCPW and SICL, a larger gap width requires a slightly larger trace width to maintain a 50 Ω characteristic impedance, leading to a decrease in conductor loss and a minor increase in dielectric loss. The most prominent influence is observed for the radiation loss in case of GCPW. Decoupling of the trace and

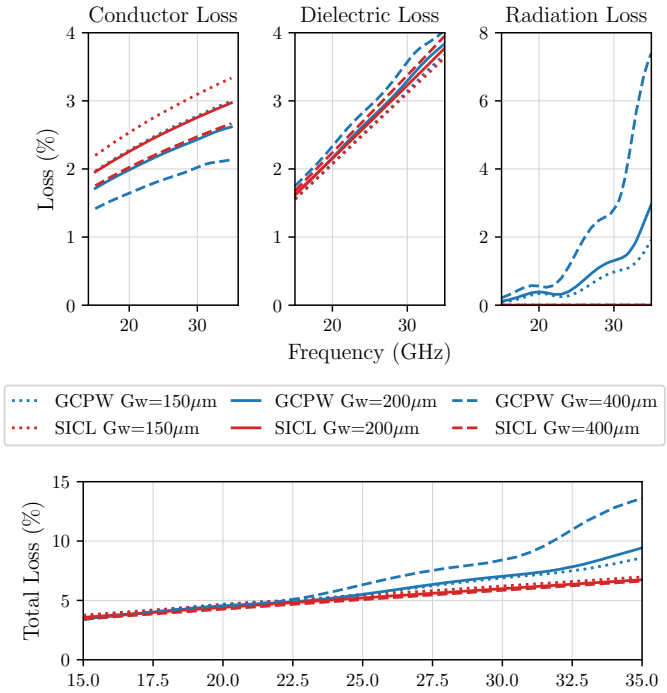

Fig. 4. Comparison of simulated (top) conductor, dielectric and radiation loss and (bottom) total loss for GCPW (blue) and SICL (red) in simulation, for several combinations of trace widths and gaps, all matched to 50 Ω.

the adjacent ground planes by making the dimensions larger, results in significantly more radiation since we evolve more towards microstrip line technology, especially above 30 GHz. Similar dielectric losses are found for the SICL and GCPW lines. Nevertheless, an increased conductor loss is expected with respect to GCPW lines, since the SICL transmission line is encapsulated by additional conducting walls and given the smaller central conductor cross-section due to the increase in effective relative permittivity. Yet, most importantly, the radiation losses were eliminated, which is especially critical at higher frequencies. Therefore, shielded transmission lines, such as SICL, become increasingly important for mmWave frequencies and beyond, as shown in Fig. 4 (bottom). Moreover, SICL implementations allow stacking multiple routing layers on top of each other without EMI issues. Simulations with a shared wall of vias between two parallel lines in the advocated SICL technology show no degradation in performance, enabling further miniaturization of the routing networks. The simulated isolation between minimally spaced parallel SICL lines remains larger than 100 dB and the total width in Fig. 1 is reduced by 0.765 mm, corresponding to a reduction of 22% in this case.

As shown in Fig. 5, the measured average insertion loss of 0.075 dB/mm in case of SICL is only slightly higher than the average 0.065 dB/mm obtained for GCPW. The slight deviation can be attributed to the ENIG surface finish, which is not included in simulation. Comparable insertion loss is demonstrated for GCPW and SICL lines. However, the SICL line shows a more compact footprint and exhibits a self-shielding property, avoiding undesired radiation or crosstalk.

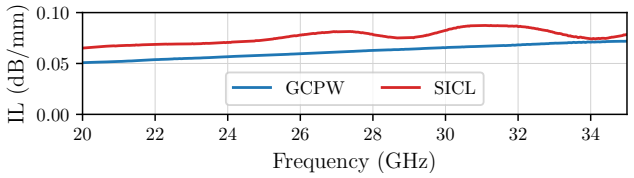

Fig. 5. Comparison of the measured losses per millimeter as a function of frequency for GCPW and SICL lines, matched to 50 Ω with Gw = 0.2 mm, integrated on a 10 mil RO4350B substrate with ENIG surface finish.

B. Coaxial Via Transition

First of all, being a fundamental component, a 50 Ω coaxial via transition is designed for minimal insertion loss. Fig. 6 shows the layout of this transition including a 1 mm-long SICL line. A photo of the four single-layer PCBs, employed to assemble the prototype, is shown on the right of Fig. 7. To enable characterization by means of a vector network analyzer (VNA, Rohde & Schwarz ZNA67), the two SICLs are interfaced by GCPW sections through coaxial transitions, integrated on PCB 1 and PCB 4. The entire test fixture, which includes the VNA's measurement cables, the 2.40 mm coaxial end-launch connectors (Southwest Microwave) mounted on PCB 1 and PCB 4, the GCPW sections and the coaxial transitions towards the short SICLs, is de-embedded by means of thru-reflect-line (TRL) calibration. As shown in Fig. 7, the TRL procedure moves the VNA's calibration planes as close as 1 mm to the actual coaxial SICL-to-SICL via transition's center, allowing accurate comparison to the simulation model, shown in Fig. 6. The resulting simulated and measured S-parameters are displayed in Fig. 8.

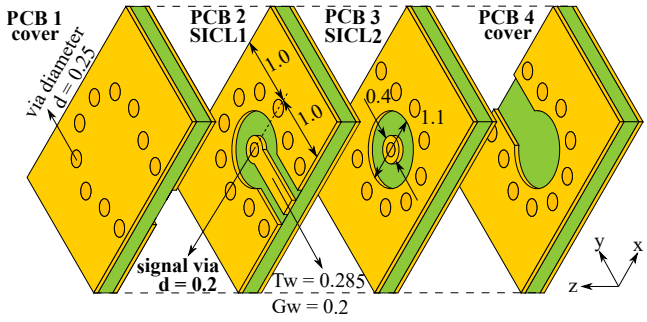

Fig. 6. Coaxial via transition from SICL to SICL with annotated dimensions in millimeter, with Tw the trace width and Gw the gap width of the SICL.

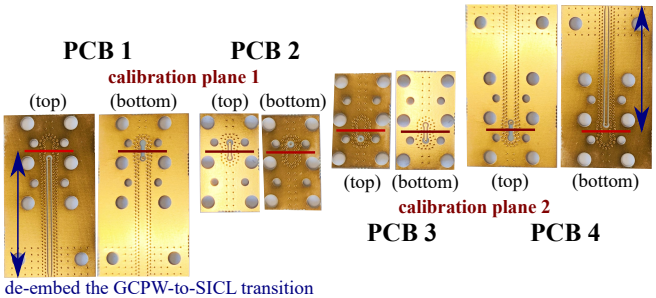

Fig. 7. Fabricated prototype parts before assembly of the coaxial via transition from SICL to SICL with annotated calibration planes in red.

The measured insertion loss remains within the range 0.55±0.15 dB from 24 GHz to 30 GHz, while the reflection coefficient stays below −13 dB. This is a slight increase compared to the simulated 0.3±0.1 dB insertion loss, caused by the surface finish, whose effect is absent in the simulation model. The proposed coaxial transition is highly suitable to realize compact routing networks, since the signal conductors on different layers may be rotated in any direction, without performance loss. To this end, the ground plane between the signal conductors on both layers and the 50 Ω-match of the coaxial via transition are crucial.

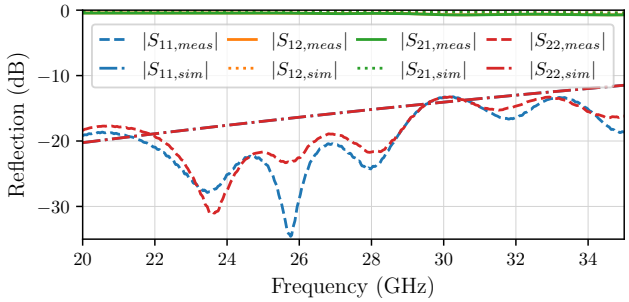

Fig. 8. SICL-to-SICL coaxial via transition: simulated (dashed-dotted) and measured (dashed) reflection coefficient; simulated (dotted) and measured (solid) transmission coefficient.

C. Hybrid Coupler

Next, we demonstrate a packaged hybrid coupler based on SICL-technology, including a transition towards GCPW for measurement purposes, as presented in Fig. 9. The component is fed by a 2.2 mm-long GCPW section, remaining after TRL calibration, which in turn transitions into a 3.5 mm-long SICL line at all four ports, before connecting to the actual hybrid coupler design. The corresponding unassembled fabricated prototype is displayed in Fig. 10.

Similar to the design procedure of a classic square branch line coupler, the impedances Z_0 of the transmission lines are initially (denoted by i) set to $Z_{0,i1} = 50\,\Omega$ and $Z_{0,i2} = Z_{0,i1}/\sqrt{2} = 35.4\,\Omega$ [29]. During optimization, a constraint is imposed on the trace width (Tw) and gap width (Gw) combinations, by fixing the total width of the trace and twice the gap for both impedances : $\mathrm{Tw}_1 + 2{\cdot}\mathrm{Gw}_1 = \mathrm{Tw}_2 + 2{\cdot}\mathrm{Gw}_2$. After optimization for minimal amplitude and phase imbalance (indicated by *opt*), we obtain a trace width of Tw = 0.3 mm and a gap width of Gw = 0.395 mm for the high-impedance lines of $Z_{0,opt1} = 50.7\,\Omega$, and we get Tw = 0.28 mm and Gw = 0.53 mm for the low-impedance lines of $Z_{0,opt2} = 35.4\,\Omega$. The core layout of the optimized quadrature hybrid coupler with dimensions indicated in millimeter is shown in the middle of Fig. 9 on the bottom conductor of PCB1. The total design, including transition lines towards GCPW for measurement purposes, fits within a footprint of 13.6 mm x 13.6 mm x 0.648 mm, which corresponds to $1.27\lambda_{0,28GHz}$ x $1.27\lambda_{0,28GHz}$ x $0.06\lambda_{0,28GHz}$ expressed as a fraction of the free space wavelength at 28 GHz, denoted as $\lambda_{0,28GHz}$.

Again, a TRL procedure is followed during the measurements to de-embed the test fixture, which includes the coaxial

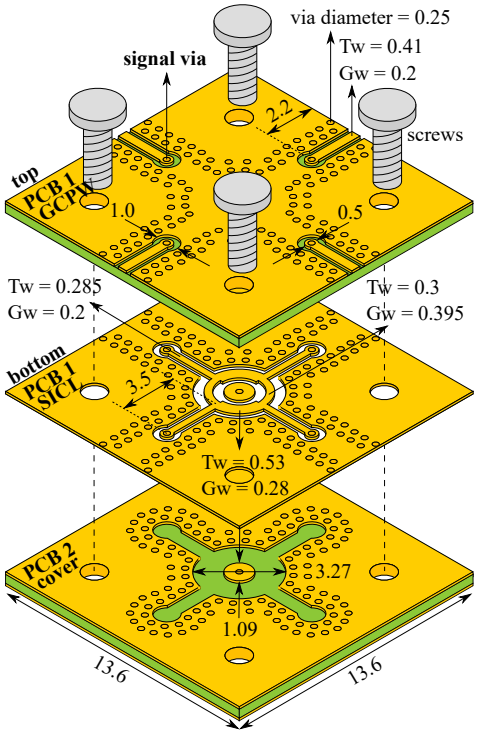

Fig. 9. Proposed SICL-based hybrid coupler transitioning to GCPW with annotated dimensions in millimeter, where Tw stands for trace width and Gw is the gap width.

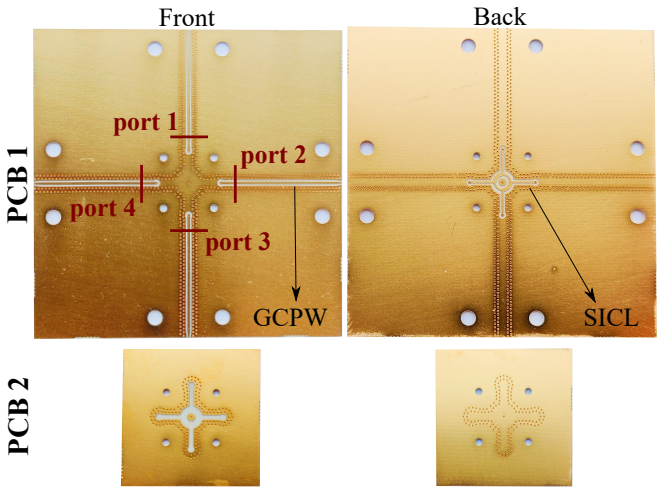

Fig. 10. Fabricated prototype parts before assembly of the proposed SICL-based hybrid coupler with GCPW transition.

end launch connectors and the extended GCPW interconnects, such that the VNA's calibration planes are located close to the device-under-test (DUT), as annotated in Fig. 10. The resulting measured S-parameters (top), amplitude imbalance and phase difference (bottom) are presented in Fig. 12. The measurements correspond very well to the simulation, with a measured excess insertion loss of $1.2\pm0.25\,\mathrm{dB}$ in the frequency band ranging from $26.5\,\mathrm{GHz}$ to $29.5\,\mathrm{GHz}$ (n257), on top of the intrinsic $3\,\mathrm{dB}$ power split loss, which is slightly higher than the simulated value of $0.7\pm0.4\,\mathrm{dB}$ due to the employed surface finish.

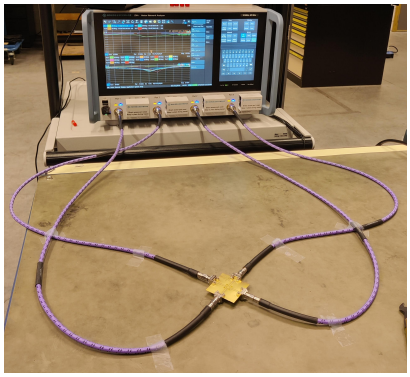

Fig. 11. Measurement setup of the assembled hybrid coupler prototype.

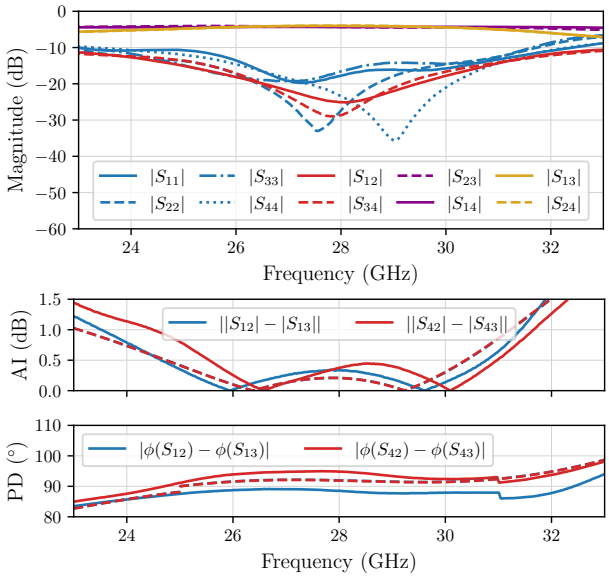

Fig. 12. (top) The measured S-parameters, (bottom) the measured (solid) and simulated (dashed) amplitude imbalance (AI) and phase difference (PD) of the hybrid coupler in SICL technology with transition to GCPW.

Simulations indicate that the influence of an air gap between the individual PCBs is negligible, since a $5\,\mu\mathrm{m}$-gap between both PCBs amounts to a maximal additional loss of $0.1\,\mathrm{dB}$ over the entire frequency range. The measured amplitude imbalance between both output ports remains smaller than $0.5\,\mathrm{dB}$ from $26.5\,\mathrm{GHz}$ to $29.5\,\mathrm{GHz}$ (n257), while the phase imbalance stays below 6°.

D. Miniaturized Hybrid Coupler

The quadrature hybrid coupler proposed in the previous subsection, which transitions towards GCPW for measurement purposes, is interesting when developing a circuit on a single SICL layer, since the different SICL components can be placed in close proximity. However, when only a single hybrid coupler is required and the available surface area is limited, which often occurs in beamsteering circuits, a more area-efficient implementation can be devised. As shown in Fig. 13, a miniaturized hybrid coupler with direct interfacing to another SICL or GCPW layer is implemented by leveraging an additional isolation PCB layer (PCB 2).

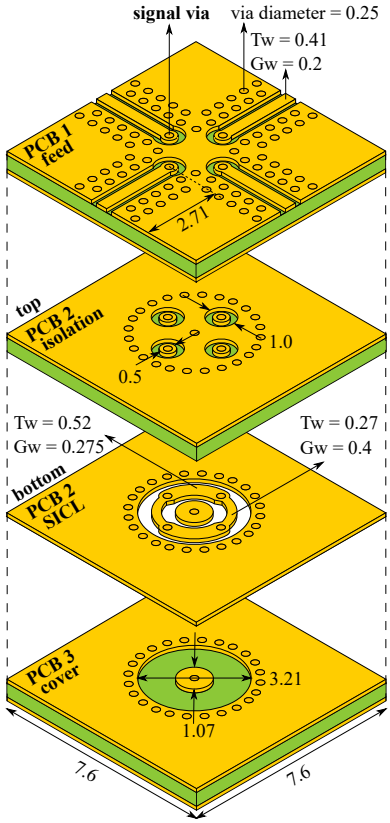

Fig. 13. Proposed miniaturized SICL-based hybrid coupler including a direct layer-transition, with annotated dimensions in millimeter, where Tw stands for trace width and Gw is the gap width.

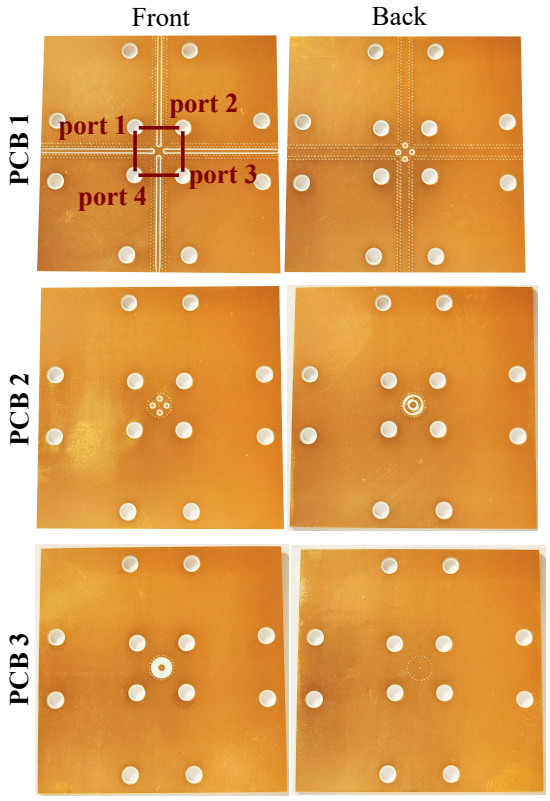

Fig. 14. Fabricated prototype parts before assembly of the proposed miniaturized SICL-based hybrid coupler.

After optimization for minimal amplitude and phase imbalance (denoted *opt*) of the proposed compact hybrid coupler topology by means of the frequency solver of CST Microwave Studio, we obtain a trace width of Tw = 0.27 mm and a gap width of Gw = 0.4 mm for the high-impedance line $Z_{0,opt1} = 53.7\,\Omega$, and we get Tw = 0.275 mm and Gw = 0.52 mm for the low-impedance line $Z_{0,opt2} = 35.8\,\Omega$. The prototype single-layer PCBs before assembly are shown in Fig. 14. After TRL de-embedding, with the port planes indicated in Fig. 14, the calibrated measurements correspond very well to the simulation results, as can be observed from Fig. 15. The measured excess insertion loss amounts to 0.8±0.3 dB from 26.5 GHz to 29.5 GHz, in addition to the intrinsic 3 dB power split. The measured reflection coefficients remain below −15 dB in this frequency range, while the input and output port isolation exceed 20 dB. The phase imbalance is smaller than 3° and the deviation from the ideal 90° phase difference between the output ports is less than 7° in all considered 28 GHz 5G bands (24.25 GHz-29.5 GHz). In this frequency range, the measured amplitude imbalance remains below 0.72 dB. The deviation is less than 2° for the n257 frequency band (26.5 GHz-29.5 GHz), where the measured amplitude imbalance stays below 0.4 dB.

The main advantage of this topology remains the completely packaged and self-shielded layout by using SICL technology, thereby avoiding EMI/EMC issues. Additionally, the direct interfacing not only minimizes the footprint to only 4 mm in diameter, but it also improves the routing flexibility significantly. Since the feed lines are completely shielded from

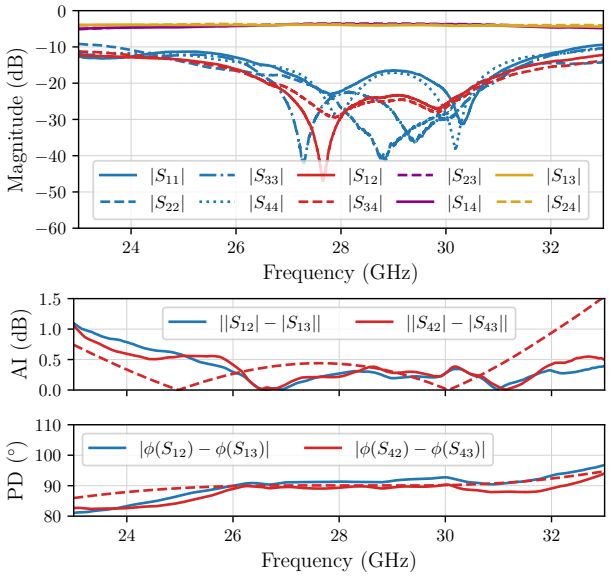

Fig. 15. (top) The measured S-parameters, (bottom) the measured (solid) and simulated (dashed) amplitude imbalance (AI) and phase difference (PD) of the miniaturized hybrid coupler.

the quadrature hybrid coupler, they can be rotated, and they can interface with the functional component from any possible angle. Moreover, when striving for extremely compact designs, the input and output signals are often routed on different PCB layers. The proposed topology can be altered slightly, such that the input lines connect from above and the output lines interface from below, without modifying the component's

characteristics. Since the miniaturized hybrid coupler is on another layer than the routing signals, an increased amount of routing space is available, simplifying the final layout process.

IV. Conclusion

This paper presented a cost-effective fabrication process to realize highly shielded substrate integrated coaxial lines (SICLs), based on the assembly of single-layer standard printed circuit boards (PCBs). Over a frequency range of $20\,\mathrm{GHz}$ to $35\,\mathrm{GHz}$, the average measured insertion loss of a SICL transmission line equals $0.075\,\mathrm{dB/mm}$, where the insertion loss is $0.065\,\mathrm{dB/mm}$ at $20\,\mathrm{GHz}$ and $0.08\,\mathrm{dB/mm}$ at $35\,\mathrm{GHz}$. The proposed SICL-to-SICL transition has a measured average insertion loss of $0.55\,\mathrm{dB}$. More specifically, the measured insertion loss amounts to $0.46\,\mathrm{dB}$ at $20\,\mathrm{GHz}$ and $0.73\,\mathrm{dB}$ at $35\,\mathrm{GHz}$.

The proposed SICL-based quadrature hybrid coupler with transition towards grounded co-planar waveguide (GCPW) for measurement purposes fits within a footprint of $12.5\,\mathrm{mm}$ x $12.5\,\mathrm{mm}$ x $0.65\,\mathrm{mm}$. It works optimally for the n257 frequency band (from $26.5\,\mathrm{GHz}$ to $29.5\,\mathrm{GHz}$), where it exhibits an excess insertion loss of $1.2 \pm 0.3\,\mathrm{dB}$, on top of the $3\,\mathrm{dB}$ power split, and a phase imbalance not exceeding 6°. This design is further miniaturized into a completely shielded hybrid coupler with direct feed interfacing, increasing the routing flexibility. The miniaturized hybrid coupler fits within a footprint of $4\,\mathrm{mm}$ x $4\,\mathrm{mm}$ x $0.97\,\mathrm{mm}$, while the measured excess insertion loss remains below $1.2 \pm 0.6\,\mathrm{dB}$ and the phase imbalance does not exceed 3° for a large frequency range from $23.75\,\mathrm{GHz}$ to $32.5\,\mathrm{GHz}$. This makes our proposed miniaturized hybrid coupler suitable for compact, broadband and cost-effective integration into future communication systems.

References

[1] F. Liu, C. Masouros, A. P. Petropulu, H. Griffiths and L. Hanzo, "Joint radar and communication design: Applications, state-of-the-art, and the road ahead," IEEE Transactions on Communications, vol. 68, no. 6, pp. 3834–3862, Feb. 2020.

[2] D. Pozar and D. Schaubert, "Scan blindness in infinite phased arrays of printed dipoles," IEEE Transactions on Antennas and Propagation, vol. 32, no. 6, pp. 602–610, Jun. 1984.

[3] K. E. Kolodziej, B. T. Perry. and J. S. Herd, "In-band full-duplex technology: Techniques and systems survey," IEEE Transactions on Microwave Theory and Techniques, vol. 67, no. 7, pp. 3025–3041, Feb. 2019.

[4] K. Wu, M. Bozzi, and N. J. G. Fonseca, "Substrate integrated transmission lines: Review and applications," IEEE Journal of Microwaves, vol. 1, no. 1, pp. 345–363, Jan. 2021.

[5] L. Van Messem et al., "Substrate integrated components for passive millimeterwave-frequency beamforming networks," 2021 IEEE MTT-S International Microwave Workshop Series on Advanced Materials and Processes for RF and THz Applications, pp. 272–274, Nov. 2021.

[6] Y. Wang, K. Ma, and Z. Jian, "A low-loss Butler matrix using patch element and honeycomb concept on SISL platform," IEEE Transactions on Microwave Theory and Techniques, vol. 66, no. 8, pp. 3622–3631, Aug. 2018.

[7] C.-C. Chang, R.-H. Lee, and T.-Y. Shih, "Design of a beam switching/steering Butler matrix for phased array system," IEEE Transactions on Antennas and Propagation, vol. 58, no. 2, pp. 367–374, Feb. 2010.

[8] F. Gatti, M. Bozzi, L. Perregrini, K. Wu, and R. G. Bosisio, "A novel substrate integrated coaxial line (SICL) for wide-band applications," 2006 European Microwave Conference, pp. 1614–1617, Sept. 2006.

[9] W. Li, J. Xu, R. Zhao and W. Hong, "Compact broadband substrate-integrated coaxial line 2-D beamforming network and its multibeam array atenna applications," IEEE Transactions on Microwave Theory and Techniques, vol. 72, no. 1, pp. 262–274, Jan. 2024.

[10] M. Cariou, B. Potelon, C. Quendo, S. Cadiou, E. Schlaffer, W. Pessl and A. Le Fevre, "Compact X-band filter based on substrate integrated coaxial line stubs using advanced multilayer PCB technology," IEEE Transactions on Microwave Theory and Techniques, vol. 65, no. 2, pp. 496–503, Dec. 2016.

[11] Q. Tan, K. Fan, F. Zhu, X. Dai, Y. Qian and G. Q. Luo, "A wideband SICL-to-waveguide transition for multilayer planar circuit applications at V-band," IEEE Microwave and Wireless Components Letters, vol. 32, no. 9, pp. 1027–1030, Apr. 2022.

[12] J. Butler and R. Lowe, "Beam-forming matrix simplifies design of electronically scanned antennas," Electron. Des., vol. 9, no. 8, pp. 170–173, Apr. 1961.

[13] L. Van Messem et al., "A 4x4 millimeterwave-frequency Butler matrix in grounded co-planar waveguide technology for compact integration with 5G antenna arrays," IEEE Transactions on Microwave Theory and Techniques, vol. 71, no. 1, pp. 122–134, June 2022.

[14] A. K. Vallappil, M. K. A. Rahim, B. A. Khawaja, N. A. Murad and M. G. Mustapha, "Butler matrix based beamforming networks for phased array antenna systems: A comprehensive review and future directions for 5G applications," IEEE Access, vol. 9, pp. 3970–3987, Jan. 2021.

[15] N. J. Fonseca, "Printed S-band 4×4 Nolen matrix for multiple beam antenna applications," IEEE transactions on antennas and propagation, vol. 57, no. 6, pp. 1673–1678, Jun. 2009.

[16] T. Djerafi, N. J. Fonseca and K. Wu, "Broadband substrate integrated waveguide 4×4 Nolen matrix based on coupler delay compensation," IEEE transactions on microwave theory and techniques, vol. 59, no. 7, pp. 1740–1745, May 2011.

[17] Y. Yang, Y. F. Pan, S. Y. Zheng, W. Hong and W. S. Chan, "Analytical design method and implementation of broadband 4x4 Nolen matrix," IEEE Transactions on Microwave Theory and Techniques, vol. 70, no. 1, pp. 343–355, Nov. 2021.

[18] I. S. Krishna and S. Mukherjee, "Design of wideband microstrip to SICL transition for millimeter-wave applications," IEEE Access, vol. 8, pp. 4250–4254, Dec. 2019.

[19] A. A. Abdulbari, S. K. A. Rahim, P. J. Soh, M. H. Dahri, A. A. Eteng, and M. Y. Zeain, "A review of hybrid couplers: State-of-the-art, applications, design issues and challenges," International Journal of Numerical Modelling: Electronic Networks, Devices and Fields, vol. 34, no. 5, pp. 1–19, May 2021.

[20] F. Gatti, M. Bozzi, L. Perregrini, K. Wu and R. G. Bosisio, "A novel substrate integrated coaxial line (SICL) for wide-band applications," 2006 European Microwave Conference, pp. 1614–1617, Sep. 2006.

[21] S.-C. Jung, R. Negra and F. M. Ghannouchi, "A design methodology for miniaturized 3-dB branch-line hybrid couplers using distributed capacitors printed in the inner area," IEEE Transactions on Microwave Theory and Techniques, vol. 56, no. 12, pp. 2950–2953, Nov. 2008.

[22] S. Reshma and M. K. Mandal, "Miniaturization of a 90° hybrid coupler with improved bandwidth performance," IEEE Microwave and Wireless Components Letters, vol. 26, no. 11, pp. 891–893, Oct. 2016.

[23] K.-Y. Tsai, H.-S. Yang, J.-H. Chen and Y.-J. E. Chen, "A miniaturized 3 dB branch-line hybrid coupler with harmonics suppression," IEEE Microwave and Wireless Components Letters, vol. 21, no. 10, pp. 537–539, Sep. 2011.

[24] S. Jun-Yu, L. Qiang, W. Yong-Le, L. Yuan-An, L. Shu-Lan, Y. Cui-Ping and L. Gan, "High-directivity single-and dual-band directional couplers based on substrate integrated coaxial line technology," 2013 IEEE MTT-S International Microwave Symposium Digest (MTT), pp. 1–4, Jun. 2013.

[25] A. Vosoogh, A. A. Brazález, Y. Li and Z. S. He, "A compact mass-producible E-band bandpass filter based on multi-layer waveguide technology," 2020 14th European Conference on Antennas and Propagation (EuCAP), pp. 1–5. IEEE, Mar. 2020.

[26] S. Yang, Z. Yu, and J. Zhou, "A low-loss broadband planar transition from ground coplanar waveguide to substrate-integrated coaxial line," IEEE Microwave and Wireless Components Letters, vol. 31, no. 11, pp. 1191–1194, Nov. 2021.

[27] L. Van Messem, A. Moerman, O. Caytan, H. Rogier and S. Lemey, "Substrate integrated coaxial line millimeterwave components manufactured in standard PCB," 2023 IEEE 32nd Conference on Electrical Performance of Electronic Packaging and Systems (EPEPS), pp. 1–3, Oct. 2023.

[28] M. Bozzi, F. Xu, D. Deslandes and K. Wu, "Modeling and design considerations for substrate integrated waveguide circuits and components," 2007 8th International Conference on Telecommunications in Modern Satellite, Cable and Broadcasting Services, pp. P-VII–P-XVI, Sept. 2007.

[29] D. M. Pozar, Microwave Engineering. John Wiley and Sons, 2011.